

---

# QD-RL: Efficient Mixing of Quality and Diversity in Reinforcement Learning

---

**Geoffrey Cideron**  
 InstaDeep  
 g.cideron@instadeep.com

**Thomas Pierrot**  
 InstaDeep  
 t.pierrot@instadeep.com

**Nicolas Perrin**  
 CNRS, Sorbonne Université  
 perrin@isir.upmc.fr

**Karim Beguir**  
 InstaDeep  
 kb@instadeep.com

**Olivier Sigaud**  
 Sorbonne Université  
 olivier.sigaud@upmc.fr

## Abstract

We propose a novel reinforcement learning algorithm, QD-RL, that incorporates the strengths of off-policy RL algorithms into Quality Diversity (QD) approaches. Quality-Diversity methods contribute structural biases by decoupling the search for diversity from the search for high return, resulting in efficient management of the exploration-exploitation trade-off. However, these approaches generally suffer from sample inefficiency as they call upon evolutionary techniques. QD-RL removes this limitation by relying on off-policy RL algorithms. More precisely, we train a population of off-policy deep RL agents to simultaneously maximize diversity inside the population and the return of the agents. QD-RL selects agents from the diversity-return Pareto Front, resulting in stable and efficient population updates. Our experiments on the ANT-MAZE environment show that QD-RL can solve challenging exploration and control problems with deceptive rewards while being more than 15 times more sample efficient than its evolutionary counterparts.

## 1 Introduction

Despite outstanding successes in specific domains such as games [40, 21] and robotics [42, 1], Reinforcement Learning (RL) algorithms are still far from being immediately applicable to complex sequential decision problems. Among the issues, a remaining burden is the need to find the right balance between exploitation and exploration. On one hand, algorithms which do not explore enough can easily get stuck in poor local optima. On the other hand, exploring too much hinders sample efficiency and can even prevent users from applying RL to large real world problems.

Dealing with this exploration-exploitation trade-off has been the focus of many RL papers [41, 4, 16, 32]. Among other things, having a population of agents working in parallel in the same environment is now a common recipe to stabilize learning and improve exploration, as these parallel agents collect a more diverse set of samples. This has led to two approaches, namely *distributed RL* where the agents are the same and *population-based training*, where diversity between agents further favors exploration [43, 29]. However, such methods do certainly not make the most efficient use of available computational resources, as the agents may collect highly redundant information.

Besides, the focus on sparse or deceptive rewards problems led to the realization that looking for diversity independently from maximizing rewards might be a good exploration strategy [24, 14, 7]. More recently, it was established that if one can define a *behavior space* or *outcome space* corresponding to the smaller space that matters to decide if a behavior is successful or not, maximizing diversity in this space might be the optimal strategy to find the sparse reward source [12].

When the reward signal is not sparse though, one can do better than just looking for diversity. Trying to simultaneously maximize diversity and rewards has been formalized into the Quality-Diversity (QD) framework [35, 9]. The corresponding algorithms try to populate the outcome space as widely as possible with an *archive* of past solutions which are both diverse and reward efficient. To do so, they generally rely on evolutionary algorithms. Selecting diverse and reward efficient solutions is then performed using the Pareto front of the *diversity*  $\times$  *reward efficiency* landscape, or populating a grid of outcome cells with reward efficient solutions in the MAP-ELITES algorithm [27]. In principle, the QD approach offers a great way to deal with the exploration-exploitation trade-off as it simultaneously ensures pressure towards both wide covering of the outcome space and high return efficiency. However, these methods suffer from relying on evolutionary methods. Though they have been shown to be competitive with deep RL approaches provided enough computational power [36, 6], they do not take advantage of the gradient’s analytical form, and thus have to sample to estimate gradients, resulting in far worse sample efficiency than their deep RL counterparts [38].

On the other hand, deep RL methods which leverage policy gradients have far better sample efficiency but they struggle on problems that require strong exploration and are sensitive to poorly conditioned reward signals such as deceptive rewards [7]. This is in part because they explore in the action space, the state-action space or the policy space rather than in an outcome space.

In this work, we combine the general QD framework with policy gradient methods and capitalize on the strengths of both approaches. Our QD-RL algorithm explores in an outcome space and thus can solve problems that simultaneously require complex exploration and high dimensional control capabilities. We investigate the properties of QD-RL by first controlling a low dimensional agent in a maze, and then addressing ANT-MAZE, a larger MUJoCo benchmark. We compare QD-RL to several recent algorithms which also combine a diversity objective and a return maximization method, namely the NS-ES family which mixes evolution strategies with novelty search [8] and the ME-ES algorithm [6] which uses MAP-ELITES to maintain a diverse and high performing population. The latter has been shown to scale well enough to also address large MUJoCo benchmarks, but we show that QD-RL is several orders of magnitude more sample efficient than these competitors.

## 2 Related Work

We consider the general context of a fully observable Markov Decision Problem (MDP)  $(\mathcal{S}, \mathcal{A}, \mathcal{T}, \mathcal{R}, \gamma)$  where  $\mathcal{S}$  is the state space,  $\mathcal{A}$  is the action space,  $\mathcal{T} : \mathcal{S} \times \mathcal{A} \rightarrow \mathcal{S}$  is the transition function,  $\mathcal{R} : \mathcal{S} \times \mathcal{A} \rightarrow \mathbb{R}$  is the reward function and  $\gamma$  is a discount factor. The exploration-exploitation trade-off being central in RL, the search for efficient exploration methods are ubiquitous in the domain. We focus on the relationship between our work and two methods: those which introduce explicit diversity into a multi-actor deep RL approach, and those which combine distinct mechanisms for exploration and exploitation.

**Diversity in multi-actor RL** Managing several actors is now a well established method to improve wall clock time and stabilize learning [22]. But including an explicit diversity criterion is a more recent trend.

The ARAC algorithm [11] uses a combination of attraction and repulsion mechanisms between good agents and poor agents to ensure diversity in a population of agents trained in parallel. The algorithm shows improvement in performance in large continuous action benchmarks such as HUMANOID-V2 and sparse reward variants. But diversity is defined in the space of policy performance thus the drive towards novel behaviors could be strengthened.

The P3S-TD3 algorithm [43] is an instance of population-based training where the parameters of the best actor are softly distilled into the rest of the population. To prevent the whole population from collapsing into a single agent, a simple diversity criterion is enforced so as to maintain a minimum distance between all agents. The algorithm shows good performance over a large set of continuous action benchmarks, including "delayed" variants where the reward is obtained only every  $K$  time steps. However, the diversity criterion they use is far from guaranteeing efficient exploration of the outcome space, particularly in the absence of reward, and it seems that the algorithms mostly benefits from the higher stability of population-based training.

With respect to P3S-TD3, the DVD algorithm [29] proposes a population-wide diversity criterion which consists in maximizing the volume between the parameters of the agents in a latent space. This criterion better limits redundancy between the considered agents.

Like our work, all these methods use a population of deep RL agents and explicitly look for diversity among these agents. However, none of them addresses deceptive reward environments such as the mazes we consider in our work. Furthermore, none of them clearly separates two components nor searches for diversity in the outcome space as QD-RL does.

**Separated exploration and exploitation mechanisms** One extreme case of the separation between exploration and exploitation is "exploration-only" methods. The efficiency of this approach was first put forward within the evolutionary optimization literature [24, 12] and then imported into the reinforcement learning literature with works such as [14] which gave rise to several recent follow-up [33, 23, 20]. These methods have proven useful in the sparse reward case, but they are inherently limited when some reward signal can be used and maximized during exploration. A second approach is sequential combination. Similarly to us, the GEP-PG algorithm [7] combines a diversity seeking component, namely *Goal Exploration Processes* [15] and a deep RL algorithm, namely DDPG [25] and shows that combining them sequentially can overcome a deceptive gradient issue. This sequential combination of exploration-then-exploitation is also present in GO-EXPLORE [13] which explores first and then memorizes the sequence to look for a high reward policy in ATARI games, and in PBCS [26] which does the same in a continuous action domain. Again, this approach is limited when the reward signal can help driving the exploration process towards a satisfactory solution.

Removing the sequentiality limitation, some approaches use a population of agents with various exploration rates [3]. Along a different line, the CEM-RL algorithm [34] combines an evolutionary algorithm, CEM [10], and a deep RL algorithm, TD3 [18] in such a way that each component takes the lead when it is the most appropriate in the current situation. Doing so, CEM-RL benefits from the better sample efficiency of deep RL and from the higher stability of evolutionary methods. But the evolutionary part is not truly a diversity seeking component and, being still an evolutionary method, it is not as sample efficient as TD3. A common feature between CEM-RL and our work is that the reward seeking agents benefit from the findings of the other agents by sharing their replay buffer.

Closer to our quality-diversity inspired approach, [8] proposes QD-ES and NSR-ES. But, as outlined in [6], these approaches are not sample efficient and the diversity and environment reward functions are mixed in a less efficient way. The most closely related work w.r.t. ours is [6]. The ME-ES algorithm also optimizes both diversity and reward efficiency, using an archive and two ES populations. Instead of using a Pareto front, ME-ES uses the MAP-ELITES approach where the outcome space is split in cells that the algorithm has to cover. Using such distributional ES approach has been shown to be critically more efficient than population-based GA methods [36], but our results show that they are still less sample efficient than off-policy deep RL methods as they do not leverage direct access to the policy gradient.

### 3 QD-RL

We present QD-RL, a quality-diversity optimization method designed to address hard exploration problems where sample efficiency matters. As depicted in Figure 1, QD-RL optimizes a population of agents for both environment reward and diversity using off-policy policy gradient methods which are known to be more efficient than traditional genetic algorithms or evolution strategies [36, 31]. In this study, we chose to rely on the TD3 agent (see Supplementary Section A) but any other off-policy agent such as SAC [19] could be used instead.

With respect to the standard MDP framework, QD-RL introduces an extra outcome space  $\mathcal{O}$  and a behavior characterization function  $b : \mathcal{S} \rightarrow \mathcal{O}$  that extracts the outcome  $o$  for a state  $s$ . The outcome of a behavior characterizes what matters about this behavior. As it often corresponds to what is needed to determine whether the behavior was successful or not, this outcome space can be equivalent to a goal space such as introduced in [37, 2]. For example, when working in a maze environment, the outcome may represent the coordinates  $(x, y)$  at the end of the trajectory of the agent, which may also be its goal. However, in contrast to UVFAs, we do not condition the policy on the outcome  $o$ . In this work, the behavior characterization function is given, as is also the case in [37, 2], and we

consider outcomes computed as a function of a single state. The more general case where it is learned or computed as a function of the whole trajectory is left for future work.

As any QD system, QD-RL manages a population of policies into an archive which contains all previously trained actors. The first generation contains a population of  $N$  neural actors  $\pi_{\theta_i} : \mathcal{S} \rightarrow \mathcal{A}$  with parameters  $\theta_i, i \in [1, N]$ . While all these actors share the same neural architecture, their weights are initialized differently. At each iteration, a selection mechanism based on the Pareto front selects  $N$  best actors from the archive containing all past agents, according to two criteria: the environment reward and a measure of novelty of the actor. To better stick to the QD framework, hereafter the former is called "quality" and the latter "diversity". If the Pareto front contains less than  $N$  actors, the whole Pareto front is selected and computed again over the remaining actors. Additional actors are sampled from the new Pareto front, and so on until  $N$  actors are sampled.

These selected actors form a new generation. Then, half of the selected actors are trained to optimize quality while the others optimize diversity. These actors with updated weights are then evaluated in the environment and added to the archive. In more details, training is performed as follows.

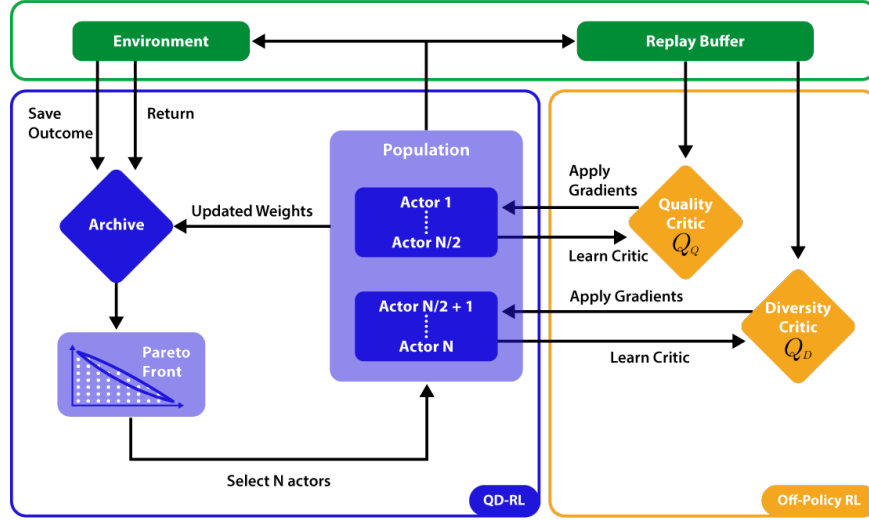


Figure 1: Architecture of the QD-RL algorithm.

First, as any standard RL method, QD-RL optimizes actors so as to maximize quality. More formally, it updates the actor weights to maximize the objective function  $J_{\text{quality}}(\theta_i) = \mathbb{E}_{\tau_i} \left[ \sum_t \gamma^t r_t^Q \right]$  where  $\tau_i$  is a trajectory obtained by following the policy  $\pi_{\theta_i}$  and  $r_t^Q = r$  is the environment reward function.

Second, QD-RL also optimizes actors to increase diversity in the outcome space. To evaluate the diversity of an outcome  $o$ , we seek for the  $k$ -nearest neighbors of outcome  $o$  in the archive and compute a novelty score  $NS(o, A)$  as the mean of the squared Euclidean distances between  $o$  and its  $k$  neighbors, as in [24, 8]. More formally, QD-RL maximizes the objective function  $J_{\text{diversity}}(\theta_i) = \mathbb{E}_{\tau_i} \left[ \sum_t \gamma^t NS(o_t, A) \right]$  where  $o_t = b(s_t)$  is the outcome discovered by policy  $i$  at time step  $t$ ,  $NS()$  is the novelty score function and  $A$  is the archive containing already discovered outcomes.

The  $J_{\text{quality}}$  and  $J_{\text{diversity}}$  functions have the same structure as we can re-write  $J_{\text{diversity}}(\theta_i) = \mathbb{E}_{\tau_i} \left[ \sum_t \gamma^t r_t^D \right]$ , where  $r_t^D = NS(o, A)$  is a non stationary reward function corresponding to novelty scores. Thus all the mechanisms introduced in the deep RL literature to optimize  $J_{\text{quality}}$  can also be applied to optimize  $J_{\text{diversity}}$ . Notably, we can introduce Q-value functions  $Q_Q$  and  $Q_D$  dealing with quality and diversity and we can define two randomly initialized critic neural networks  $Q_{\theta_Q}$  and  $Q_{\theta_D}$ , with parameters  $\theta_Q$  and  $\theta_D$  to approximate these functions. These critics are shared by all the trained actors. Therefore, they capture the average population performance rather than the performance of

individual actors, which has both an information sharing effect and a smoothing effect. We found that training individual critics is harder in practice and left this analysis for future work.

The quality and diversity update of actor weights is performed according to Equation (2). An update consists in sampling a batch of transitions from the replay buffer and optimizing the weights of both critics so as to maximize quality and diversity. Then, we optimize parameters of half policies so as to maximize  $J_{\text{quality}}$  and the other half to maximize  $J_{\text{diversity}}$ . Therefore, the global update can be written

$$\begin{cases} \theta^Q \leftarrow \theta^Q - \frac{2\alpha}{N} \nabla_{\theta^Q} \sum_{\text{batch}} \sum_{i=1}^{N/2} \left( Q_{\theta^Q}(s_t, a_t) - (r_t^Q + \gamma Q_{\theta^{Q'}}(s_{t+1}, \pi_{\theta_i}(s_{t+1}))) \right)^2 \\ \theta^D \leftarrow \theta^D - \frac{2\alpha}{N} \nabla_{\theta^D} \sum_{\text{batch}} \sum_{i=N/2+1}^N \left( Q_{\theta^D}(s_t, a_t) - (r_t^D + \gamma Q_{\theta^{D'}}(s_{t+1}, \pi_{\theta_i}(s_{t+1}))) \right)^2 \end{cases} \quad (1)$$

$$\begin{cases} \theta_i \leftarrow \theta_i + \alpha \nabla_{\theta_i} \sum_{\text{batch}} Q_{\theta^Q}(s_t, \pi_{\theta_i}(s_t)), \quad \forall i \leq N/2 \text{ // Quality update of half actors} \\ \theta_i \leftarrow \theta_i + \alpha \nabla_{\theta_i} \sum_{\text{batch}} Q_{\theta^D}(s_t, \pi_{\theta_i}(s_t)), \quad \forall i > N/2 \text{ // Diversity update of half actors} \end{cases} \quad (2)$$

where  $\theta^{Q'}$  and  $\theta^{D'}$  correspond to the parameters of target critic networks. To keep notations simple, updates of the extra critic networks introduced in TD3 to reduce the value estimation bias do not appear in (1), but we use them in practice.

Once updates have been performed, trajectories are collected in parallel from all policies. These trajectories are stored into a common replay buffer and the tuple (final outcome  $o_T$ , return, parameters) is stored into the archive. Since the novelty score of an outcome varies through time as the archive grows, instead of storing it, we store outcomes and fresh diversities are computed every time a batch is sampled from the replay buffer.

A short version of the QD-RL algorithm is presented in Algorithm 1. Other implementation details are presented in Supplementary Section B.

---

**Algorithm 1:** QD-RL (short version)

---

**Given:**  $N$ , gradient\_steps

**Initialize:** Archive  $A$ , Replay Buffer  $\mathcal{B}$ ,  $N$  actors  $\{\pi_{\theta_i}\}_{i=\{1,\dots,N\}}$ , 2 critics  $Q_{\theta^D}$  and  $Q_{\theta^Q}$

---

```
// In parallel
Evaluate in parallel the initial population to fill archive and buffer

while True do
    // Select new generation
    Compute the Pareto Front from the archive  $A$ 
    Get  $N$  actors  $\pi_{\theta_i}, i \in \{1, \dots, N\}$  from the Pareto front

    // In parallel
    for  $i \leftarrow 1$  to gradient_steps do
        Sample batch of  $(s_t, a_t, o_t, r_t, s_{t+1})$  from  $\mathcal{B}$ 
        Update first half of the population to maximise diversity
        Update second half of the population to maximise quality
        Update shared quality and diversity critics
    end

    // In parallel
    Evaluate the updated actors and fill archive and buffer
end
```

---

## 4 Experiments

In this section, we demonstrate the capability of QD-RL to solve challenging exploration problems. We implement it with the TD3 algorithm and refer to this implementation as the QD-TD3 algorithm.

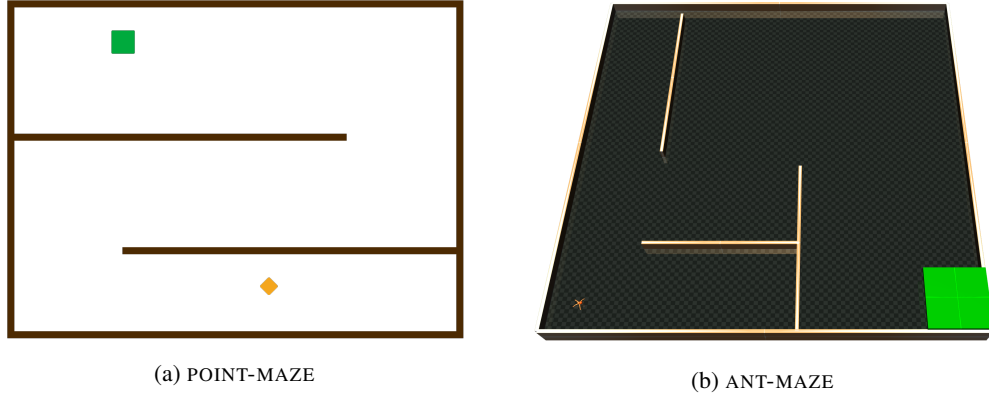


Figure 2: Experimental environments. Though they may look similar, the POINT-MAZE environment state and action spaces are two-dimensional, whereas in ANT-MAZE, the state space has 29 dimensions and the action space 8.

Hyper-parameters are described in Section B of the supplementary document. We first analyse each component of QD-TD3 and demonstrate their usefulness on a toy example. Then we show that QD-TD3 can solve a more challenging control and exploration problem such as navigating the MUJoCo Ant into a large maze with a better sample complexity than its standard evolutionary competitors.

#### 4.1 Point Maze: Move a point in a Maze

We first consider the POINT-MAZE environment in which the agent controls a 2D material point which must exit from a three corridors maze depicted in Figure 2a. The observation corresponds to the agent coordinates  $(x_t, y_t) \in [-1, 1]^2$  at time  $t$ . The two continuous actions  $(\delta x, \delta y) \in [-0.1, 0.1]^2$  correspond to position increments along the  $x$  and  $y$  axes. The outcome space is the final state  $(x_f, y_f)$  of the agent, as in [8]. The initial position of the agent is sampled uniformly in  $[-0.1, 0.1] \times [-1, -0.7]$ . This zone is located at the bottom right of the maze. The exit area is a square centered at  $(x_{\text{goal}} = -0.5, y_{\text{goal}} = 0.8)$  of width 0.1. Once this exit square is reached, the episode ends. The maximum length of an episode is 200 time steps. The reward is computed as  $r_t = -(x_t - x_{\text{goal}})^2 - (y_t - y_{\text{goal}})^2$ . This reward leads to a deceptive gradient signal: following it would lead the agent to stay stuck by the second wall in the maze, as shown in Figure 4 of Supplementary Section C. In order to exit the maze, the agent must find the right balance between exploitation and exploration, that is at a certain point ignore the policy gradient and only explore the maze. Thus, though this example may look simple due to its low dimension, it remains very challenging for standard deep reinforcement agents such as TD3.

QD-TD3 performs three main operations: (i) it optimizes half of the agents to maximize quality; (ii) it does the same to the other half to maximize diversity; (iii) it uses a quality-diversity Pareto front as a population selection mechanism. We investigate the impact of each of these components separately through an ablation study. For all experiments, we use 4 actors. Results are aggregated in Figure 3a.

First, we measure performance when training the 4 actors to maximize quality only. We call the resulting agent Q-TD3, but this is simply a multi-actor TD3. As depicted in Figure 5 of Supplementary Section C, the Q-TD3 population finds a way to the second maze wall but is stuck there due to the deceptive nature of the gradient. This experiment shows clearly enough that using a quality-only strategy has no chance of solving hard exploration problems with a deceptive reward signal such as POINT-MAZE or ANT-MAZE.

Then, we evaluate the agent performance when training the 4 actors to maximize diversity only. We call the resulting agent D-TD3. We show that D-TD3 finds sometimes how to get further the second wall but with a large variance and without finding the optimal trajectory.

We then consider a D-TD3 + PARETO agent that optimizes only for diversity but performs agent selection from the archive with a Pareto front, that is it selects 4 actors for the next generation based

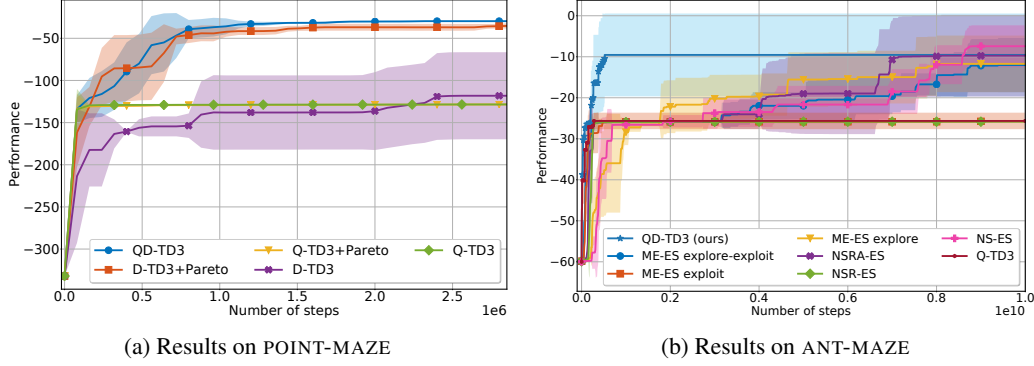


Figure 3: Learning curves of QD-TD3 versus ablations on POINT-MAZE and several other agents on ANT-MAZE. The performance corresponds to the highest return on POINT-MAZE and to the highest negative distance to the goal area on ANT-MAZE.

on both their quality and diversity, but without optimizing the former. Interestingly, adding the Pareto front selection mechanism significantly improves performance and stability.

Finally, QD-TD3 optimizes half of the actors for quality, the other half for diversity and it selects them with the Pareto Front mechanism. We observe that QD-TD3 outperforms all ablations, even if the improvement over D-TD3 + PARETO is lesser, which means that optimizing for quality is less critical in this environment as good enough solutions are found just by maximising diversity. Table 1 summarises all the ablations we performed.

	Opt. Quality	Opt. Diversity	Pareto selection	Episode return ( $\pm$ std)
QD-TD3	✓	✓	✓	-29 ( $\pm 1$ )
D-TD3 + PARETO	X	✓	✓	-35 ( $\pm 3$ )
D-TD3	X	✓	X	-111 ( $\pm 59$ )
Q-TD3 + PARETO	✓	X	✓	-128 ( $\pm 0$ )
Q-TD3	✓	X	X	-128 ( $\pm 0$ )

Table 1: Summary of compared ablations.

## 4.2 Ant Maze: Control an articulated Ant to solve a Maze

We then test QD-TD3 on a challenging environment modified from OpenAI Gym [5] based on ANT-V2 and also used in [6, 17]. We refer to this environment as the ANT-MAZE environment. In ANT-MAZE, a four-legged "ant" robot has to reach a goal zone located at  $[35, -25]$  which corresponds to the lower right part of the maze (colored in green in Figure 2b). The initial position of the ant is sampled from a small circle of radius 0.1 around the initial point  $[-25, -25]$  situated in the extreme bottom right of the maze. Maze walls are organized so that following the gradient of distance to the goal drives the ant into a dead-end. As in the POINT-MAZE, the reward is expressed as minus the distance between the center of gravity of the ant and the center of the goal zone, thus leading to a strongly deceptive gradient. This environment is more complex than POINT-MAZE as the agent must learn to control a body with 8 degrees of freedom in all directions to explore the maze and solve it. Therefore, this problem is much harder than the standard ANT-V2 gym environment in which the ant only learns to go straight forward. The observation space contains the positions, angle, velocities and angular velocities of most ant articulations and center of gravity, and has 29 dimensions. The action space is  $[-1, 1]^8$  where an action correspond to the choice of 8 continuous torque intensities to apply to the 8 ant articulations. The episodes have a fixed length of 3000 time steps. As previously, the outcome is computed as the final position  $(x_f, y_f)$  of the center of gravity of the ant.

We compare the performance of QD-TD3 on this benchmark to 4 state-of-the art methods: NSR-ES, NSRA-ES, NS-ES and ME-ES. While NS-ES and ME-ES-EXPLORE optimize only for diversity, and ME-ES-EXPLOIT optimizes only for quality, NSR-ES, NSRA-ES and ME-ES-EXPLORE-EXPLOIT optimize for both. To ensure fair comparison, we did not implement our own versions of these

algorithms but reused results from the ME-ES paper [6]. We also ensured that the environment we used was rigorously the same.

All the baselines were run for 5 seeds. In QD-TD3, each seed corresponds to 20 actors distributed on 20 CPU cores. As in [6], we compute the average and standard deviation between the seeds of the minimum distance to the goal reached at the end of an episode by one of the agents and report the results in Figure 3b. As explained in [6], NSR-ES and ME-ES-EXPLOIT obtain a score around -26, which means that they get stuck in the dead-end, similarly to Q-TD3. By contrast, all other algorithms manage to avoid it. More importantly, the QD-TD3 algorithm achieves a similar score to these better exploring agents, but in more than **15 times less samples** than its evolutionary competitors, as shown in Table 2.

	<b>Final Perf. (<math>\pm</math> std)</b>	<b>Sampled steps</b>	<b>Steps to -10</b>	<b>Ratio to QD-TD3</b>
QD-TD3 (Ours)	-10 ( $\pm 10.1$ )	6e8	5e8	1
NS-ES	-9 ( $\pm 5.6$ )	1e10	8e9	16
NSR-ES	-27 ( $\pm 0$ )	1e10	$\infty$	$\infty$
NSRA-ES	-10 ( $\pm 11$ )	1e10	8e9	16
ME-ES- EE	-10 ( $\pm 6$ )	1e10	9e9	18
ME-ES- EXPLORE	-11.7 ( $\pm 6.9$ )	1e10	9e9	18
ME-ES- EXPLOIT	-25.8 ( $\pm 0$ )	1e10	$\infty$	$\infty$
Q-TD3	-26 ( $\pm 2$ )	3e8	$\infty$	$\infty$

Table 2: Summary of compared algorithms. The mean performance is computed as the average over 5 seeds of the minimum distance to the goal reached at the end of an episode by the population. "Steps to -10" correspond to the number of steps to reach an average performance of -10. ME-ES- EE stands for ME-ES- EXPLORE-EXPLOIT.

These results show that QD-TD3 leveraged the sample efficiency brought by off-policy policy gradient to learn to efficiently explore the maze. We also emphasize the low cost of QD-TD3 compared to its evolutionary counterparts. To solve the ANT-MAZE, QD-TD3 **requires only 2 days of training on 20 CPU cores** with no GPU while evolutionary algorithms are usually run on much larger infrastructures. For instance, ME-ES needs to sample 10.000 different set of parameters per iteration and evaluates them all to compute a diversity gradient with CEM [6]. Besides, the failure of the Q-TD3 ablation into ANT-MAZE unsurprisingly shows that a pure RL approach without a diversity component fails in these deceptive gradient benchmarks.

## 5 Conclusion

In this paper, we proposed a novel way to deal with the exploration-exploitation trade-off by combining a reward-seeking component, a diversity-seeking component and a selection component inspired from the Quality-Diversity approach. Crucially, we showed that quality and diversity could be optimized with off-policy reinforcement learning algorithms, resulting in a significantly improved sample efficiency. We showed experimentally the effectiveness of the resulting QD-RL framework, which can solve in two days with 20 CPUs problems which were previously out of reach without a much larger infrastructure.

Key components of QD-RL are selection through a Pareto front and the search for diversity in an outcome space. Admittedly, the outcome space needed to compute the diversity reward is hard coded. There are attempts to automatically obtain the outcome space through unsupervised learning methods [30, 28], but defining such a space is often a trivial decision which helps a lot, and can alleviate the need to carefully design reward functions.

In the future, we first want to address the case where the outcome depends on the whole trajectory. Next we plan to further study the versatility of our approach to exploration compared to other deep reinforcement learning exploration approaches. Besides, we intend to show that our approach could be extended to problems where the environment reward function can itself be decomposed into several loosely dependent components, such as standing, moving forward and manipulating objects for a humanoid or solving multiagent reinforcement learning problems. In such environments, we could



replace the maximization of the sum of reward contributions with a multi-criteria selection from a Pareto front where diversity would be only one of the considered criteria.

## Broader Impact

Our paper presents a novel approach to the combination of diversity-driven exploration and modern reinforcement learning techniques. It results in more stable learning with respect to standard reinforcement learning, and more sample efficient learning with respect to standard evolutionary approaches to diversity. We believe this has a positive impact in making reinforcement learning techniques more accessible and feasible towards real world applications. Besides, our work may help casting a needed bridge between the reinforcement learning and the evolutionary optimization research communities. Finally, by releasing our code, we believe that we help efforts in reproducible science and allow the wider community to build upon and extend our work in the future.

## Acknowledgements

Work by Nicolas Perrin was partially supported by the French National Research Agency (ANR), Project ANR-18-CE33-0005 HUSKI.

## References

- [1] Ilge Akkaya, Marcin Andrychowicz, Maciek Chociej, Mateusz Litwin, Bob McGrew, Arthur Petron, Alex Paino, Matthias Plappert, Glenn Powell, Raphael Ribas, et al. Solving rubik’s cube with a robot hand. *arXiv preprint arXiv:1910.07113*, 2019.
- [2] Marcin Andrychowicz, Filip Wolski, Alex Ray, Jonas Schneider, Rachel Fong, Peter Welinder, Bob McGrew, Josh Tobin, Pieter Abbeel, and Wojciech Zaremba. Hindsight Experience Replay. *arXiv preprint arXiv:1707.01495*, 2017.
- [3] Adrià Puigdomènech Badia, Bilal Piot, Steven Kapturowski, Pablo Sprechmann, Alex Vitvitskyi, Daniel Guo, and Charles Blundell. Agent57: Outperforming the atari human benchmark. *arXiv preprint arXiv:2003.13350*, 2020.
- [4] Marc Bellemare, Sriram Srinivasan, Georg Ostrovski, Tom Schaul, David Saxton, and Remi Munos. Unifying count-based exploration and intrinsic motivation. In *Advances in Neural Information Processing Systems*, pages 1471–1479, 2016.
- [5] Greg Brockman, Vicki Cheung, Ludwig Pettersson, Jonas Schneider, John Schulman, Jie Tang, and Wojciech Zaremba. Openai gym. *arXiv preprint arXiv:1606.01540*, 2016.
- [6] Cédric Colas, Joost Huizinga, Vashisht Madhavan, and Jeff Clune. Scaling map-elites to deep neuroevolution. *arXiv preprint arXiv:2003.01825*, 2020.
- [7] Cédric Colas, Olivier Sigaud, and Pierre-Yves Oudeyer. GEP-PG: Decoupling exploration and exploitation in deep reinforcement learning algorithms. *arXiv preprint arXiv:1802.05054*, 2018.
- [8] Edoardo Conti, Vashisht Madhavan, Felipe Petroski Such, Joel Lehman, Kenneth O. Stanley, and Jeff Clune. Improving exploration in evolution strategies for deep reinforcement learning via a population of novelty-seeking agents. *arXiv preprint arXiv:1712.06560*, 2017.
- [9] Antoine Cully and Yiannis Demiris. Quality and diversity optimization: A unifying modular framework. *IEEE Transactions on Evolutionary Computation*, 2017.
- [10] P-T. De Boer, D.P Kroese, S. Mannor, and R.Y. Rubinstein. A tutorial on the cross-entropy method. *Annals of Operations Research*, 134(1):19–67, 2005.
- [11] Thang Doan, Bogdan Mazouze, Audrey Durand, Joelle Pineau, and R Devon Hjelm. Attraction-repulsion actor-critic for continuous control reinforcement learning. *arXiv preprint arXiv:1909.07543*, 2019.
- [12] Stephane Doncieux, Alban Laflaquière, and Alexandre Coninx. Novelty search: a theoretical perspective. In *Proceedings of the Genetic and Evolutionary Computation Conference*, pages 99–106, 2019.
- [13] Adrien Ecoffet, Joost Huizinga, Joel Lehman, Kenneth O Stanley, and Jeff Clune. Go-explore: a new approach for hard-exploration problems. *arXiv preprint arXiv:1901.10995*, 2019.

- [14] Benjamin Eysenbach, Abhishek Gupta, Julian Ibarz, and Sergey Levine. Diversity is all you need: Learning skills without a reward function. *arXiv preprint arXiv:1802.06070*, 2018.
- [15] Sébastien Forestier, Yoan Mollard, and Pierre-Yves Oudeyer. Intrinsically motivated goal exploration processes with automatic curriculum learning. *arXiv preprint arXiv:1708.02190*, 2017.
- [16] Meire Fortunato, Mohammad Gheshlaghi Azar, Bilal Piot, Jacob Menick, Ian Osband, Alex Graves, Vlad Mnih, Remi Munos, Demis Hassabis, Olivier Pietquin, et al. Noisy networks for exploration. *arXiv preprint arXiv:1706.10295*, 2017.
- [17] Kevin Frans, Jonathan Ho, Xi Chen, Pieter Abbeel, and John Schulman. Meta learning shared hierarchies. *Proc. of ICLR*, 2018.
- [18] Scott Fujimoto, Herke van Hoof, and Dave Meger. Addressing function approximation error in actor-critic methods. *arXiv preprint arXiv:1802.09477*, 2018.
- [19] Tuomas Haarnoja, Aurick Zhou, Kristian Hartikainen, George Tucker, Sehoon Ha, Jie Tan, Vikash Kumar, Henry Zhu, Abhishek Gupta, Pieter Abbeel, and Sergey Levine. Soft actor-critic algorithms and applications, 2018.
- [20] Riashat Islam, Zafarali Ahmed, and Doina Precup. Marginalized state distribution entropy regularization in policy optimization. *arXiv preprint arXiv:1912.05128*, 2019.
- [21] Max Jaderberg, Wojciech M Czarnecki, Iain Dunning, Luke Marris, Guy Lever, Antonio Garcia Castaneda, Charles Beattie, Neil C Rabinowitz, Ari S Morcos, Avraham Ruderman, et al. Human-level performance in 3d multiplayer games with population-based reinforcement learning. *Science*, 364(6443):859–865, 2019.
- [22] Max Jaderberg, Valentin Dalibard, Simon Osindero, Wojciech M Czarnecki, Jeff Donahue, Ali Razavi, Oriol Vinyals, Tim Green, Iain Dunning, Karen Simonyan, et al. Population-based training of neural networks. *arXiv preprint arXiv:1711.09846*, 2017.
- [23] Lisa Lee, Benjamin Eysenbach, Emilio Parisotto, Eric Xing, Sergey Levine, and Ruslan Salakhutdinov. Efficient exploration via state marginal matching. *arXiv preprint arXiv:1906.05274*, 2019.
- [24] Joel Lehman and Kenneth O. Stanley. Abandoning objectives: Evolution through the search for novelty alone. *Evolutionary computation*, 19(2):189–223, 2011.
- [25] Timothy P Lillicrap, Jonathan J Hunt, Alexander Pritzel, Nicolas Heess, Tom Erez, Yuval Tassa, David Silver, and Daan Wierstra. Continuous control with deep reinforcement learning. *arXiv preprint arXiv:1509.02971*, 2015.
- [26] Guillaume Matheron, Nicolas Perrin, and Olivier Sigaud. Pbc: Efficient exploration and exploitation using a synergy between reinforcement learning and motion planning. *arXiv preprint arXiv:2004.11667*, 2020.
- [27] Jean-Baptiste Mouret and Jeff Clune. Illuminating search spaces by mapping elites. *arXiv preprint arXiv:1504.04909*, 2015.
- [28] Giuseppe Paolo, Alban Laflaquiere, Alexandre Coninx, and Stephane Doncieux. Unsupervised learning and exploration of reachable outcome space. *algorithms*, 24:25, 2019.
- [29] Jack Parker-Holder, Aldo Pacchiano, Krzysztof Choromanski, and Stephen Roberts. Effective diversity in population-based reinforcement learning. *arXiv preprint arXiv:2002.00632*, 2020.
- [30] Alexandre Péré, Sébastien Forestier, Olivier Sigaud, and Pierre-Yves Oudeyer. Unsupervised learning of goal spaces for intrinsically motivated goal exploration. *arXiv preprint arXiv:1803.00781*, 2018.
- [31] Felipe Petroski Such, Vashisht Madhavan, Edoardo Conti, Joel Lehman, Kenneth O. Stanley, and Jeff Clune. Deep neuroevolution: Genetic algorithms are a competitive alternative for training deep neural networks for reinforcement learning. *arXiv preprint arXiv:1712.06567*, 2017.
- [32] Matthias Plappert, Rein Houthoofd, Prafulla Dhariwal, Szymon Sidor, Richard Y. Chen, Xi Chen, Tamim Asfour, Pieter Abbeel, and Marcin Andrychowicz. Parameter space noise for exploration. *arXiv preprint arXiv:1706.01905*, 2017.
- [33] Vitchyr H Pong, Murtaza Dalal, Steven Lin, Ashvin Nair, Shikhar Bahl, and Sergey Levine. Skew-fit: State-covering self-supervised reinforcement learning. *arXiv preprint arXiv:1903.03698*, 2019.
- [34] Aloïs Pourchot and Olivier Sigaud. Cem-rl: Combining evolutionary and gradient-based methods for policy search. *arXiv preprint arXiv:1810.01222*, 2018.

- [35] Justin K Pugh, Lisa B Soros, and Kenneth O. Stanley. Quality diversity: A new frontier for evolutionary computation. *Frontiers in Robotics and AI*, 3:40, 2016.
- [36] Tim Salimans, Jonathan Ho, Xi Chen, and Ilya Sutskever. Evolution strategies as a scalable alternative to reinforcement learning. *arXiv preprint arXiv:1703.03864*, 2017.
- [37] Tom Schaul, Daniel Horgan, Karol Gregor, and David Silver. Universal value function approximators. In *International Conference on Machine Learning*, pages 1312–1320, 2015.
- [38] Olivier Sigaud and Freek Stulp. Policy search in continuous action domains: an overview. *Neural Networks*, 113:28–40, 2019.
- [39] David Silver, Guy Lever, Nicolas Heess, Thomas Degris, Daan Wierstra, and Martin Riedmiller. Deterministic policy gradient algorithms. In *Proceedings of the 30th International Conference in Machine Learning*, 2014.
- [40] David Silver, Julian Schrittwieser, Karen Simonyan, Ioannis Antonoglou, Aja Huang, Arthur Guez, Thomas Hubert, Lucas Baker, Matthew Lai, Adrian Bolton, et al. Mastering the game of go without human knowledge. *Nature*, 550(7676):354–359, 2017.
- [41] Haoran Tang, Rein Houthoofd, Davis Foote, Adam Stooke, Xi Chen, Yan Duan, John Schulman, Filip De Turck, and Pieter Abbeel. # exploration: A study of count-based exploration for deep reinforcement learning. *arXiv preprint arXiv:1611.04717*, 2016.
- [42] Josh Tobin, Lukas Biewald, Rocky Duan, Marcin Andrychowicz, Ankur Handa, Vikash Kumar, Bob McGrew, Alex Ray, Jonas Schneider, Peter Welinder, et al. Domain randomization and generative models for robotic grasping. In *2018 IEEE/RSJ International Conference on Intelligent Robots and Systems (IROS)*, pages 3482–3489. IEEE, 2018.
- [43] Youngchul Sung, Whiyung Jung, Giseung Park. Population-guided parallel policy search for reinforcement learning. In *International Conference on Learning Representations*, 2020.

## Appendices

### A The TD3 Agent

The Twin Delayed Deep Deterministic (TD3) agent [18] builds upon the Deep Deterministic Policy Gradient (DDPG) agent [25]. It trains a deterministic actor  $\pi_\phi : \mathcal{S} \rightarrow \mathcal{A}$  that maps directly environment observations to continuous actions and a critic  $Q_\theta : \mathcal{S} \times \mathcal{A} \rightarrow \mathbb{R}$  that takes an environment state  $s$  and an action  $a$  and estimates the average return from selecting action  $a$  in state  $s$  and then following policy  $\pi_\phi$ . DDPG alternates policy evaluation and policy improvement operations so as to maximise the average discounted return. In DDPG, the critic is updated to minimize a temporal difference error during the policy evaluation step which induces an overestimation bias. TD3 corrects for this bias by introducing two critics  $Q_{\theta_1}$  and  $Q_{\theta_2}$ . TD3 alternates between interactions with the environment and critic and actor updates. It plays one step in the environment using its deterministic policy and then stores the observed transition  $(s_t, a_t, r_t, s_{t+1})$  into a replay buffer  $\mathcal{B}$ . Then, it samples a batch of transitions from  $\mathcal{B}$  and updates the critic networks. Half the time it also samples another batch of transitions to update the actor network.

Both critics are updated so as to minimize a loss function which is expressed as a mean squared error between their predictions and a target:

$$L^{critic}(\theta_1, \theta_2) = \sum_{\text{batch}} (Q_{\theta_1}(s_t, a_t) - y_t)^2 + (Q_{\theta_2}(s_t, a_t) - y_t)^2, \quad (3)$$

where the common target  $y_t$  is computed as:

$$y_t = r_t + \gamma \min_{i=1,2} Q_{\theta_i}(s_{t+1}, \pi_\phi(s_{t+1}) + \epsilon), \quad \epsilon \sim \mathcal{N}(0, I). \quad (4)$$

The Q-value estimation used to compute target  $y_t$  is taken as minimum between both critic predictions thus reducing the overestimation bias. TD3 also adds a small perturbation  $\epsilon$  to the action  $\pi_\phi(s_{t+1})$  so as to smooth the value estimate by bootstrapping similar state-action value estimates.

Every two critics updates, the actor  $\pi_\phi$  is updated using the deterministic policy gradient also used in DDPG [39]. For a state  $s$ , DDPG updates the actor such as to maximise the critic estimation for this state  $s$  and the action  $a = \pi_\phi(s)$  selected by the actor. As there are two critics in TD3, the authors suggest to take the first critic as an arbitrary choice. Thus, the actor is updated by minimizing the following loss function:

$$L^{actor}(\phi) = - \sum_{\text{batch}} Q_{\theta_1}(s_t, \pi_\phi(s_t)). \quad (5)$$

Policy evaluation and policy improvement steps are repeated until convergence. TD3 demonstrates state of the art performance on some MUJoCo benchmarks. In this study, we use it to update the population of actors for both quality and diversity.

### B QD-RL Implementation Details

In POINT-MAZE, the dimensions of the state space and the action space are both equal to 2. By contrast, in ANT-MAZE the dimension of the state space is 29 while the action space dimension is 8. We use fully connected layers networks for all actors and critics.

We consider populations of  $N = 4$  actors for the POINT-MAZE environment and  $N = 20$  actors for the ANT-MAZE environment. We use 1 CPU thread per actor. The code parallelisation is implemented with the Message Passing Interface (MPI) library. Our experiments were run on a machine with 20 CPU cores and 100 GB of RAM. We did not use any GPU. One experiment on the POINT-MAZE takes between 2 and 3 hours while an experiment on the ANT-MAZE takes 2 days.

During one iteration of the QD-RL algorithm, the actors of the population are updated according to Equation (2) where the losses are computed on batches sampled from a shared replay buffer. Then, the actors are evaluated. All the gradients are computed in parallel. Then, the gradients relative to

the critic networks are averaged through a reduce operation and redistributed to the actors threads to update their weights.

After being updated, actors are evaluated by performing an episode. Evaluations also take place in parallel. All the transitions  $(s_t, a_t, o_t, r_t, s_{t+1})$  are stored into a replay buffer. For each actor, we also compute the discounted return over the episode as  $R = \sum_{t=0}^T \gamma^t r_t$  where  $T$  is the episode length. We compute the distance between the final outcome  $o_T$  and its closest neighbor in the archive. If this distance is superior to an acceptance threshold (see below for values), we add the tuple (actor set of weights, return  $R$ , final outcome  $o_T$ ) to the archive. Otherwise, we decide between keeping the new actor or its closest neighbor in the archive by selecting the one with the highest return. This selection technique, suggested in [9], allows QD-RL to save space by only keeping the relevant elements. We also set a maximum size for the archive. If this maximum was to be reached we would use a First In First Out mechanism. However it was never the case in any of our experiments.

Finally, to select the new actors from the population to start the next iteration, we compute a quality-diversity Pareto Front of all the actors saved in the archive. We sample the  $N$  actors in the Pareto Front. If the Pareto front contains less than  $N$  actors, we select them all, remove them, compute the Pareto front over the remaining actors and sample again from it, and so on until we get  $N$  actors.

### B.1 Hyper-parameters

We summarize all the hyper-parameters used in experiments in Table 3. We highlight the fact that most of these hyper-parameters values are the original ones for the TD3 algorithm. Our method introduces only 3 hyper-parameters: the archive size, the threshold of acceptance to add an outcome in the archive and the  $k$  nearest neighbors. The archive size value is determined to never be reached. We found that QD-RL is not sensitive to the number  $k$  of nearest neighbors as long as this number is higher than 5. The threshold of acceptance is determined to find a good trade-off between keeping an archive of an acceptable size with respect to the infrastructure RAM capacities and not being too selective so as to keep a maximum number of meaningful actors set of weights.

Parameter	Point Maze	Ant Maze
<b>Reinforcement Learning</b>		
optimizer	Adam	Adam
learning rate	$3.10^{-4}$	$3.10^{-4}$
discount factor $\gamma$	0.99	0.99
replay buffer size	$10^6$	$5.10^5$
hidden layers size	64/32	256/256
activations	ReLU	ReLU
minibatch size	256	256
target smoothing coefficient	0.005	0.005
delay policy update	2	2
target update interval	1	1
gradient steps	1	0.005
<b>Archive</b>		
archive size	10000	10000
threshold of acceptance	0.0001	0.1
k nearest neighbors	10	10

Table 3: QD-TD3 Hyper-parameters

## B.2 Full Pseudo Code of QD-RL

---

### Algorithm 2: QD-RL (extended version)

---

**Given:**  $N$ ,  $\text{max\_steps}$ ,  $\text{gradient\_steps\_ratio}$ ,

**Initialize:** Archive  $A$ , Replay Buffer  $\mathcal{B}$ ,  $N$  actors  $\{\pi_{\theta_i}\}_{i=\{1,\dots,N\}}$ , 2 critics  $Q_{\theta^D}$  and  $Q_{\theta^Q}$

```

total_steps, actor_steps = 0, 0 // Step counters

// Evaluate in parallel the initial population to fill archive and buffer
for j ← 1 to N do
    Play one episode with actor  $\pi_{\theta_j}$ 
    Get episode length  $T$ , discounted return  $R$  and final outcome  $o_T$ 
    Store collected transitions in  $\mathcal{B}$ 
    Add the tuple  $(R, o_T, \theta_j)$  in the archive  $A$ 
    actor_steps ← actor_steps +  $T$ 
end

// Algorithm main loop
while total_steps < max_steps do
    // Select new generation
    Compute the Pareto Front from the archive  $A$ 
    Get the  $N$  actors  $\pi_{\theta_i}, i \in \{1, \dots, N\}$  from the Pareto front
    gradient_steps = int(actor_steps × gradient_steps_ratio)
    actor_steps = 0

    // Perform in parallel population update and evaluation
    for j ← 1 to N do
        // Update the population
        for i ← 1 to gradient_steps do
            Sample batch of  $(s_t, a_t, o_t, r_t, s_{t+1})$  from  $\mathcal{B}$ 

            // First half is updated to maximise diversity
            if j ≤ N/2 then
                Compute novelty reward as  $r_t^D = N(o_t, A)$ 
                Update  $\pi_{\theta_j}: \theta_j \leftarrow \theta_j + \nabla J_{\text{diversity}}(\theta_j)$ 
                Compute novelty critic gradient locally
                Averaged between parallel thread novelty critic gradients
                Update novelty critic  $Q_{\theta^D}$ 
            end

            // Second half is updated to maximise quality
            else
                Update  $\pi_{\theta_j}: \theta_j \leftarrow \theta_j + \nabla J_{\text{quality}}(\theta_j)$ 
                Compute quality critic gradient locally
                Averaged between parallel thread quality critic gradients
                Update quality critic  $Q_{\theta^Q}$ 
            end
        end

        // Evaluate the updated actors
        Play one episode with actor  $\pi_{\theta_j}$ 
        Get episode length  $T$ , discounted return  $R$  and final outcome  $o_T$ 
        Store collected transitions in  $\mathcal{B}$ 
        Add the tuple  $(R, o_T, \theta_j)$  in the archive  $A$ 
        actor_steps ← actor_steps +  $T$ 
    end

    total_steps ← total_steps + actor_steps // Update total time steps
end

```

---

## C Point-Maze and Ant-Maze Environments analysis

In this section, we propose a finer analysis of the POINT-MAZE and ANT-MAZE environments. We highlight why these environments are hard to solve for classical deep RL agents without extra exploration mechanisms and show the impact of the different components of our algorithm.

### C.1 Deceptive Gradient in Ant-Maze

Figure 4, highlights the deceptive nature of the ANT-MAZE environment reward by depicting gradient fields in both environments.

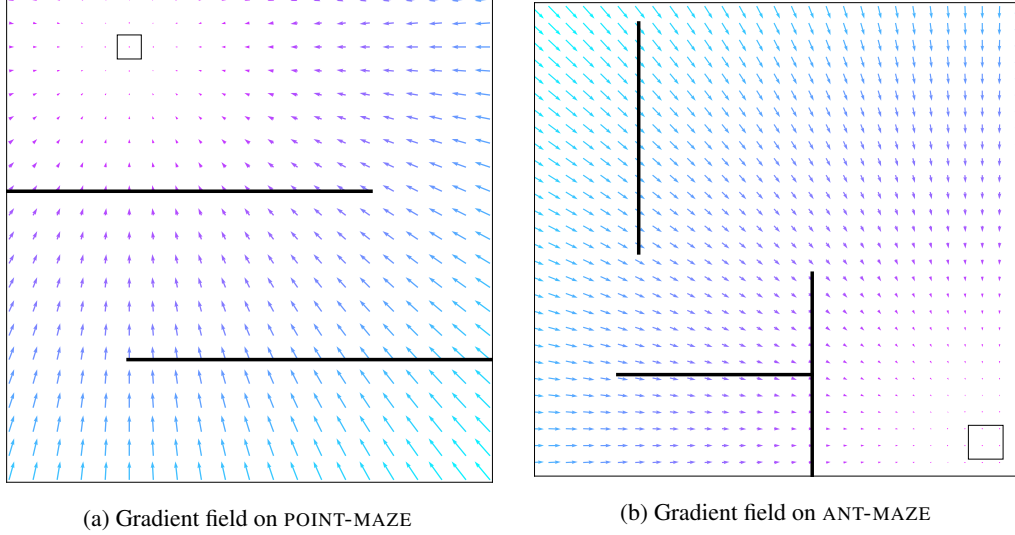


Figure 4: Gradients maps.

### C.2 Exploration in Point-Maze for All Ablations

Figure 5 summarizes the coverage of the POINT-MAZE environment by the different ablation algorithms over the course of training. A dot in the figure corresponds to the final position of an agent performing an episode in the environment. The color highlights the course of training: agents evaluated early in training are in blue while newer ones are represented in purple. Figure 5 corresponds to the map coverage for one seed, we chose the most representative among all seeds. As D-TD3 suffers from a high variance between seeds, we showed two possible behaviors: one where the whole map is covered and one where D-TD3 gets stuck.

In Figure 5, all algorithms using diversity (QD-TD3, D-TD3, D-TD3 + PARETO) are able to explore the whole environment. The lower region, full of blue dots, is explored first while the upper region, full of purple dots, is explored later. In the map coverage of QD-TD3, the area in the right corner just above the first wall is not explored. This is because QD-TD3 favors both quality and diversity so this area is not explored in priority. The two algorithms relying on quality only (Q-TD3 and Q-TD3 + PARETO) quickly reach the first wall and then get stuck here because of the deceptive reward signal.

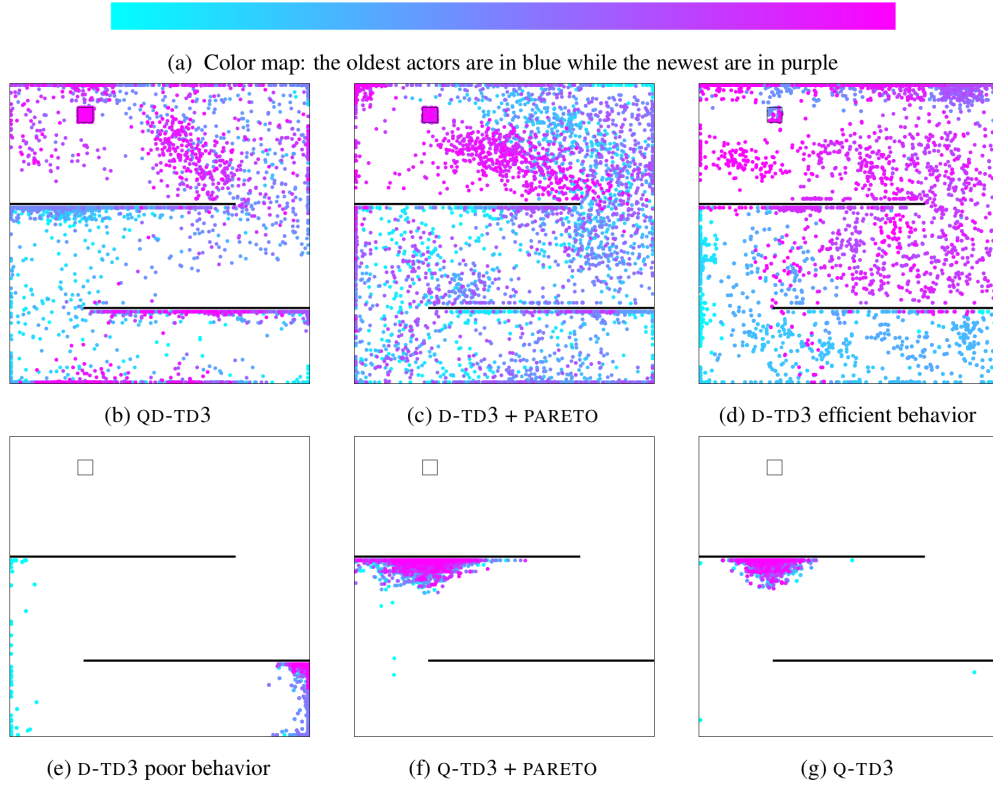


Figure 5: Coverage map of the POINT-MAZE for each of QD-TD3 ablations. Each dot corresponds to the position of an actor at the end of an episode. Dots corresponding to the oldest actors are in blue while the newest are in purple.